ELSEVIER

Journal of Wind Engineering
and Industrial Aerodynamics 89 (2001) 947–966

JOURNAL OF wind engineering AND industrial aerodynamics

www.elsevier.com/locate/jweia

Two-dimensional numerical modeling of flow and dispersion in the presence of hill and buildings

Jae-Jin Kim[a], Jong-Jin Baik[a,*], Hye-Yeong Chun[b]

[a] *Department of Environmental Science and Engineering, Kwangju Institute of Science and Technology, 1 Oryong-dong, Puk-gu, Kwangju 500-712, South Korea*

[b] *Department of Atmospheric Sciences and Global Environment Laboratory, Yonsei University, Seoul 120-749, South Korea*

Abstract

A two-dimensional numerical model with a k–ε turbulence closure scheme and a non-uniform grid system is used to examine the effects of a single hill and/or two buildings on the flow and pollutant dispersion. In a single-hill configuration, the hill slope is an important factor determining the existence of a recirculation zone behind the hill. As the hill slope increases, the recirculation zone becomes wide. In the presence of a single street canyon formed by two isolated buildings, the ambient wind blows not parallel to the roof-level but passes above the canyon with a small curvature. This results in more momentum transfer into the street canyon by the ambient wind than that in a slot-flow case. When there exist both a single hill and two buildings, the vertical velocity at the top height of the canyon becomes negligible as the height of the downwind street canyon approaches to that of the upwind hill. A flow reattachment promoted by the upwind hill acts to restrict the vertical extent of vortex below the roof-level and to enlarge the size of recirculation zone behind the downwind building. The obstacle effects on pollutant plume dispersion are examined by analyzing the vertical standard deviation and average height of plume. The upward motion induced by flow impingement influences plume height in front of the obstacles, while behind them the downward motion related to flow reattachment to the ground largely affects the vertical spread and average height of plume. In the presence of both a single hill and two buildings, an accelerated reattachment at the top height of the canyon by the upwind hill plays an important role in the vertical spread and average height of plume.

Keywords: Recirculation zone; Flow reattachment; Flow impingement; Vertical plume spread; Average plume height

*Corresponding author. Tel.: +82-62-970-2437; fax: +82-62-970-2434.
E-mail address: jjbaik@aromi.kjist.ac.kr (J.-J. Baik).

0167-6105/01/$ - see front matter
PII: S0167-6105(01)00092-7

1. Introduction

A highly industrial and/or traffic-congested urban area has serious air pollution problems. To minimize possible damages by air pollution, it is necessary to reduce pollutant emission and to predict air quality accurately. Air pollution in an urban area is linked closely to meteorology and local topography. A systematic study of flow and dispersion in the presence of a simple topography is the first step toward a better understanding of flow and dispersion in a complex urban terrain.

During the past several decades, there have been extensive theoretical, numerical, and experimental studies of changes in mean flow and turbulence structure caused by topography. Theoretical models based on a mixing-length approach [1,2] are adequate for determining mean-flow change but have limitations in determining topographic effects on turbulence structure. When a current of air passes over an obstacle, a recirculation zone can be formed behind the obstacle. Whether a recirculation zone can be produced or not depends largely on obstacle slope [3,4]. Factors affecting the horizontal and vertical scales of recirculation zone, which are a great concern to air pollution researchers, include flow stratification, upstream wind shear and turbulence intensity, obstacle shape, and so on. A wind-tunnel study of Castro and Robins [5] showed that an increase in incident wind shear and turbulence intensity weakens recirculation zone. A numerical study of Zhang et al. [6] supported their result. The mean-flow advection has been known as an effective process of pollutant transport over a hill-shaped obstacle in a laminar flow [7] and under a strong stable flow [8] due to a decrease in turbulence intensity. The effect of flow stratification in a microscale system may not be as essential as in a topographically forced mesoscale system, because it can be neglected in the building wake due to the dominant shear-generated mechanical turbulence [9].

Although complex arrays with various types of obstacles exist in a real urban area, many authors have been interested in flow and pollutant dispersion in a single hill or a single building or two buildings. This paper particularly aims at understanding flow and pollutant dispersion when both a hill and a street canyon formed by two buildings are present. The effects of a single hill or a street canyon are examined first and then results are compared with those obtained in the presence of both a hill and a canyon. For this, a two-dimensional numerical model which employs a k–ε turbulence closure scheme is used.

2. Numerical model and experimental setup

The numerical model used in this study is the same as that described by Baik and Kim [10], except that a non-uniform grid system is implemented in the model. The numerical model is a two-dimensional (x–z), nonhydrostatic, nonrotating, and incompressible model with a k–ε turbulence closure scheme. The governing equations are solved on a staggered grid system using a finite volume method [11]. For further details of the model, see Baik and Kim [10].

Four obstacle configurations are considered in this study (Fig. 1): no obstacle, a single hill (Fig. 1a), two buildings (Fig. 1b), and a single hill and two buildings (Fig. 1c). The cases of Fig. 1b and c will be called single street-canyon and dual-obstacle cases, respectively. The hill is cosine square shaped and its center is located at $x = 254.1$ m. The height of the hill (H_h) is fixed at 10.2 m but its bottom width (W_h) varies (52.9, 65.3, 82.6, and 113.6 m). Corresponding maximum hill slopes are 31.3°, 26.2°, 21.3°, and 15.8°, respectively. Two isolated buildings with equal heights form a street canyon. The width of both the upwind and downwind buildings (W_b) is set to 23.6 m. The width between the two buildings (W_c) is fixed at 23.2 m. The building height (H_c) varies with 5.3, 10.2, 15.6, and 21.5 m, giving street aspect ratios (H_c/W_c) of 0.23, 0.44, 0.67, and 0.93, respectively. According to the numerical studies of street-canyon flows [10,12–14], three flow regimes (isolated roughness flow, wake interference flow, and skimming flow) should be observed in this range of aspect ratios. The center of the street canyon is located at $x = 360.7$ m.

A non-uniform grid system with 190 cells in the horizontal and 82 cells in the vertical is used. The smallest cell dimension is 0.5 m in the horizontal and 0.2 m in the vertical, which is situated at the hill crest. From the hill crest, the grid interval

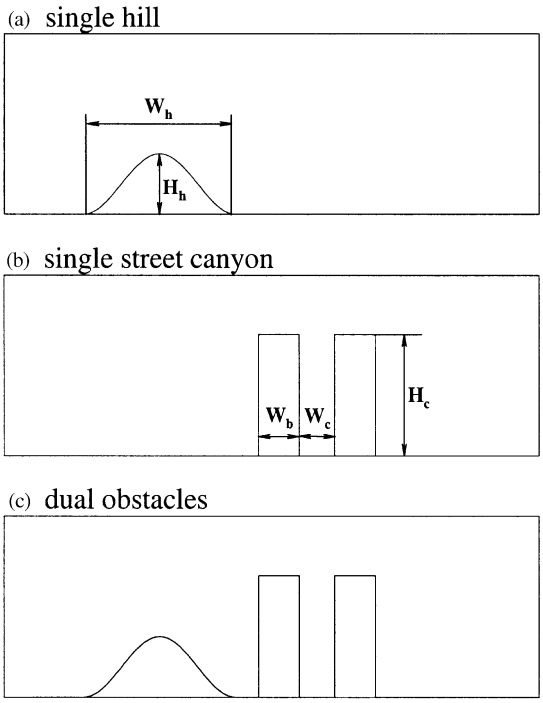

Fig. 1. The model obstacle configurations: (a) a single hill, (b) two buildings, and (c) a single hill and two buildings.

uniformly increases upwind and upward until it equals 9.6 and 10.0 m, respectively, and increases downward to the ground. To simulate street-canyon flow reasonably well, the horizontal grid interval increases downwind from the hill crest until it is equal to 6.0 m and decreases until it equals 1.9 m. Then, the horizontal grid interval increases until it equals 9.6 m and then remains constant. The expansion ratio in this non-uniform grid system is 1.1. Castro and Apsley [15] used an expansion ratio of 1.07 and Zhang et al. [8] used expansion ratios not exceeding 1.3. The horizontal and vertical domain sizes are 1239.1 and 311.7 m, respectively. The specified inflow horizontal velocity has a power-law profile ($U_i = U_r(z/z_r)^{0.299}$, where $U_r = 2.5$ m s^{-1} and $z_r = 10$ m). The inflow turbulent kinetic energy and its dissipation are specified following Castro and Apsley [15]. The time step is 0.5 s.

3. Results and discussion

3.1. Flow analyses

Fig. 2 shows the streamline fields at $t = 2$ h in the presence of a single hill. The hill-bottom width (W_h) is variant with 113.6, 82.6, 65.3, and 52.9 m (denoted by H1, H2, H3, and H4, respectively). In the H1 and H2 cases with maximum hill slopes of 15.8° and 21.3°, respectively, a recirculation zone behind the hill is not produced. However, in the H3 and H4 cases with maximum hill slopes of 26.2° and 31.3°, respectively, a recirculation zone appears. This result is consistent with the field observation of Mason and King [3], the wind-tunnel measurement of Arya and Gadiyaram [4], and the numerical study of Castro and Apsley [15]. In these studies, a well-defined recirculation zone is formed behind a hill with respective slopes of 24.0°, 26.5°, and 26.0°. Our result is, however, different from that in Britter et al. [16] which showed that an intermittent recirculation zone is observed behind a bell-shaped hill with a maximum hill slope of 14.6°. The horizontal length of recirculation zone is 24 m ($2.4H_h$) in the H3 case and 28 m ($2.7H_h$) in the H4 case. This is in good agreement with the wind-tunnel result ($2.5H_h$) for a conical hill with a slope of 26.5° of Arya and Gadiyaram [4], although Castro and Snyder [17] pointed out that a two-dimensional ridge with the same hill slope as a three-dimensional conical hill makes a longer recirculation zone. Note that the hill in this study has a smoother crest than that of Arya and Gadiyaram [4].

Flow is separated at a hill crest and the recirculation zone becomes wider as the shape of hill crest is sharper. Arya and Shipman [18] reported that the horizontal and vertical lengths of recirculation zone behind a triangular ridge with a slope of 63.4° are $13.0H_h$ and $2.5H_h$, respectively. The horizontal length of recirculation zone in this study ($2.4H_h$ in the H3 case and $2.7H_h$ in the H4 case) is much smaller than that in their study. This is because the shape of hill crest in this study is not as sharp as a triangular ridge and the hill is less steeper than that in their study.

In this study, a rectangular coordinate system was employed to take rectangular buildings into account. Accordingly, the hill was inevitably represented by a stair-stepped structure (a smooth hill shape was drawn in Figs. 1, 2, 6, and 8 only for a

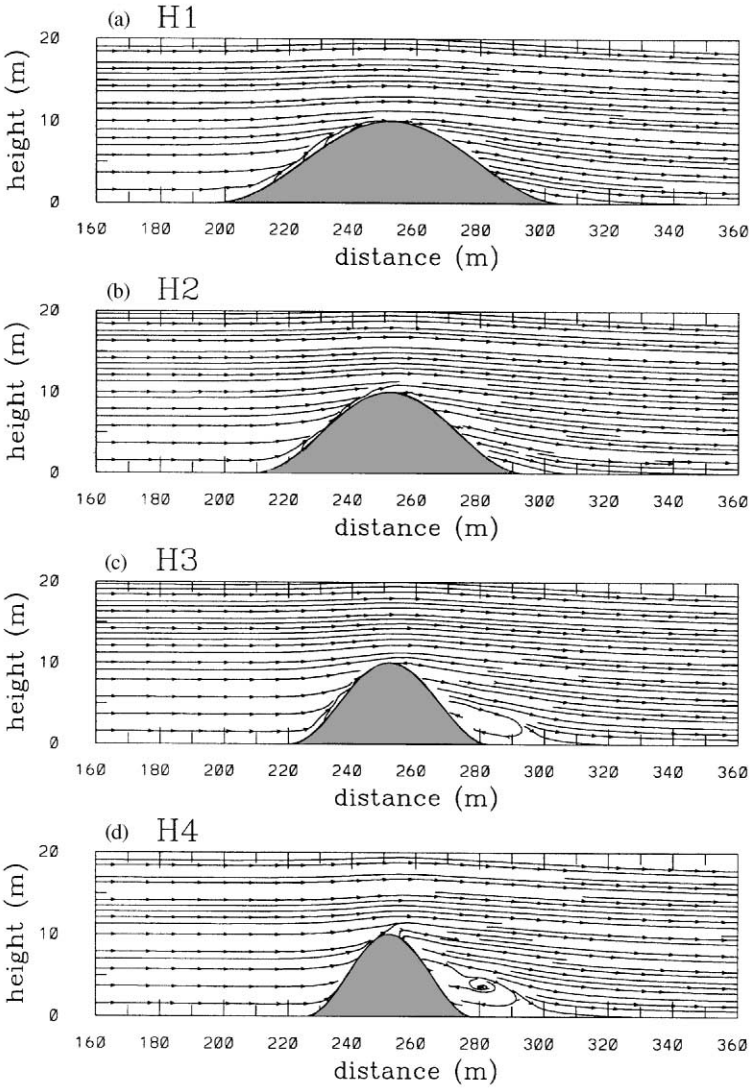

Fig. 2. The streamline fields at $t = 2$ h for hill-bottom widths (W_h) of (a) 113.6 (H1), (b) 82.6 (H2), (c) 65.3 (H3), and (d) 52.9 m (H4) in a single-hill configuration.

display purpose). Therefore, the streamlines near the hill can be strangely broken (see Fig. 2). Of course, if one uses a terrain-following coordinate system, the streamline close to the hill follows the hill shape. However, with this coordinate system, one cannot properly represent buildings.

Fig. 3 shows the vertical profiles of the fractional speed-up factor at a hill crest. The speed-up factor (S) and fractional speed-up factor (ΔS) can be represented,

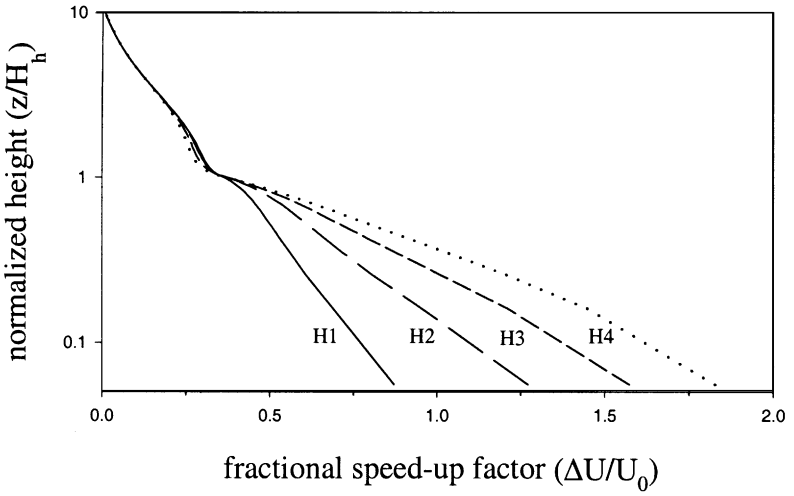

Fig. 3. The vertical profiles of the fractional speed-up factor at a hill crest at $t = 2$ h in the H1, H2, H3, and H4 cases in a single-hill configuration. The vertical axis is in a log-scale.

respectively, as

$$S = 1 + \Delta S, \tag{1}$$

$$\Delta S = [U(z + H_h) - U_0(z)]/U_0(z), \tag{2}$$

where $U(z + H_h)$ is the horizontal velocity at height z above a hill crest and $U_0(z)$ is the far-upstream velocity at height z above the flat terrain. For $U_0(z)$, the vertical profile at a location of about 190 m distant upwind from the upwind hill-base is used. The maximum fractional speed-up factors computed in the H1, H2, H3, and H4 cases are 0.87, 1.27, 1.57, and 1.83, respectively, and in all the cases they appear at $z = 0.056H_h$. Castro and Apsley [15] reported a maximum fractional speed-up factor of 1.15 for a two-dimensional bell-shaped hill with a maximum slope of 26.0°. This value is smaller than that in the H3 case (1.57).

In a theoretical study of flow over a gentle hill behind which a flow separation does not occur, Jackson and Hunt [1] found that the speed-up factor is determined by the hill shape and slope. In particular, in the case of a two-dimensional hill, the speed-up factor is a function of slope parameter (H/L) and can be expressed by [4]

$$S = 1 + a\frac{H}{L}, \tag{3}$$

where H is the hill height and L is the half-length scale of hill (streamwise distance from the crest to the half-height point). The coefficient a in (3) is approximately 2. The speed-up factors calculated using (3) in the H1 ($H/L = 0.36$), H2 (0.49), H3 (0.63), and H4 (0.77) cases are 1.72, 1.98, 2.26, and 2.54, respectively. The maximum speed-up factors in the numerical-model simulations are larger than those

computed using (3). A linear fit between S and H/L using the numerical-model results gives $a = 2.44$, which is larger than that given by Arya and Gadiyaram [4].

Next, flow field, when there exist two isolated buildings, is examined and the street-canyon flow in this open configuration is compared with that in a closed configuration (slot flow). Fig. 4 shows the streamline fields for aspect ratios of 0.23, 0.44, 0.67, and 0.93 (denoted by C1, C2, C3, and C4, respectively). When the aspect

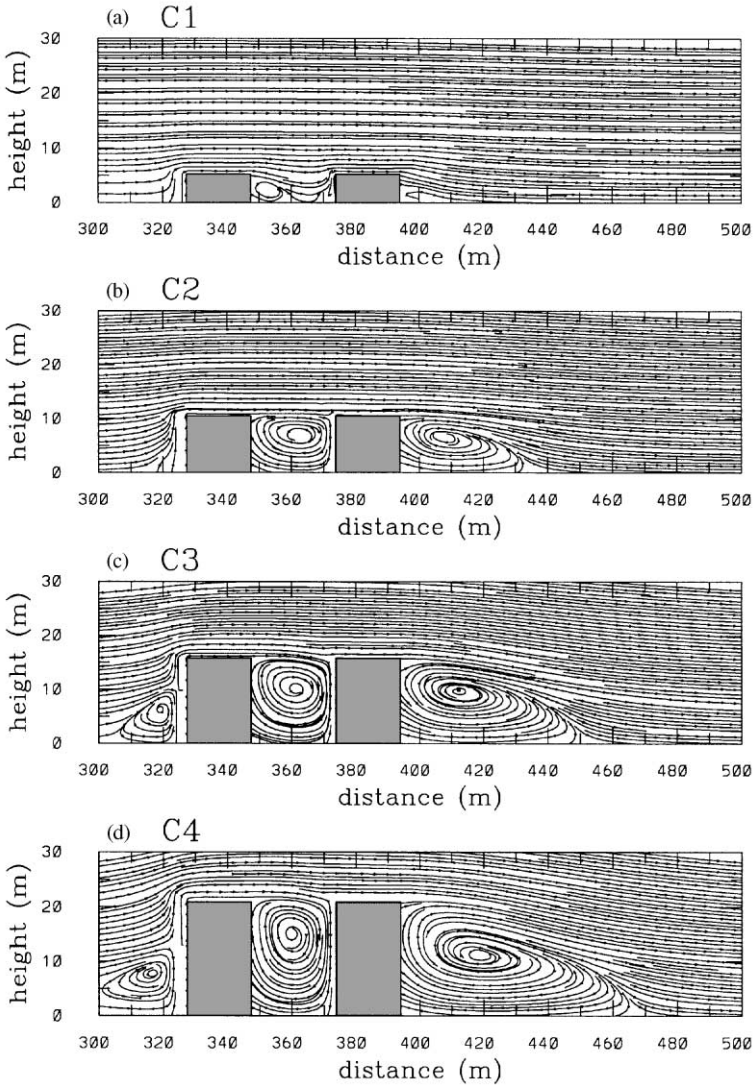

Fig. 4. The streamline fields at $t = 2$ h for aspect ratios (H_c/W_c) of (a) 0.23 (C1), (b) 0.44 (C2), (c) 0.67 (C3), and (d) 0.93 (C4) in a single street-canyon configuration.

ratio is 0.23, isolated roughness flow is observed in the canyon. For an aspect ratio of 0.44, it is somewhat ambiguous to identify a flow regime. However, it is true that the vortex formed in the canyon takes characteristics of wake interference flow according to the criteria of Hunter et al. [12]. Skimming flow is observed when the aspect ratio is 0.67 and 0.93. These results are in good agreement with previous studies of flow regimes in street canyons [12,14,19] which indicate that isolated roughness, wake interference, and skimming flows are observed in ranges of $H_c/W_c < \sim 0.33$, $\sim 0.33 < H_c/W_c < \sim 0.67$, and $H_c/W_c > \sim 0.67$, respectively.

As for the pollutant dispersion, one of the important features to be considered is a recirculation zone produced behind the downwind building. The horizontal lengths of recirculation zone in the C1, C2, C3, and C4 cases are 6 ($1.1H_c$), 38 ($3.7H_c$), 54 ($3.5H_c$), and 72 m ($3.3H_c$), respectively. The horizontal length in each of the C2, C3, and C4 cases is larger than that ($2.7H_c$) corresponding to a neutral condition in a three-dimensional numerical study of Zhang et al. [8]. From a wind-tunnel experiment of Castro and Snyder [17], it is expected that the horizontal length of recirculation zone is longer in a two-dimensional simulation than in a three-dimensional simulation.

To examine the effect of grid interval and structure on simulated flow field, an experiment was performed in which the horizontal grid interval was set to 0.8 m in the region between ~ 65 m upwind and ~ 130 m downwind from the center of the street canyon but other experimental setting was the same as in the C4 experiment. The simulated flow field in this experiment with a finer horizontal resolution was similar to that in the C4 experiment. For example, the horizontal length of recirculation zone behind the downwind building decreased by only 2 m.

Previous numerical studies (e.g. [14]) of street-canyon flows were carried out for the slot-flow case (hereafter, closed street-canyon case) in which a main concern was flow within a canyon. The situation considered in this study is named the open street-canyon case because two buildings forming a street canyon stand up in an open domain. A large difference between open and closed street-canyon cases can be found near the top height of a canyon, especially in a skimming flow. Main characteristics of skimming flow in a closed street-canyon case are that the vertical extent of vortex is restricted below the roof-level of a canyon and that the wind direction above the canyon is parallel to the roof-level. However, in an open street-canyon case, the ambient wind blows not parallel to the roof-level but passes above the canyon with a small curvature due to an upward deviation of the ambient wind by flow impingement near the leading edge of an upwind building. As a result, the vertical extent of vortex can exceed a roof-level. In this study, the width of buildings (W_b) is narrow so that a wind deviation by the upwind building can largely influence flow within the canyon. However, if the width is wide enough for a flow to reattach on the building roof, the ambient wind parallel to the roof-level should be generated [20].

Fig. 5 illustrates the vertical profiles of the normalized horizontal and vertical velocities near the upwind and downwind buildings and at the center of the street canyon for aspect ratios of 0.44 and 0.93. These aspect ratios are close to those in Baik and Kim [10] (0.5 and 1). The reverse horizontal velocity in the open

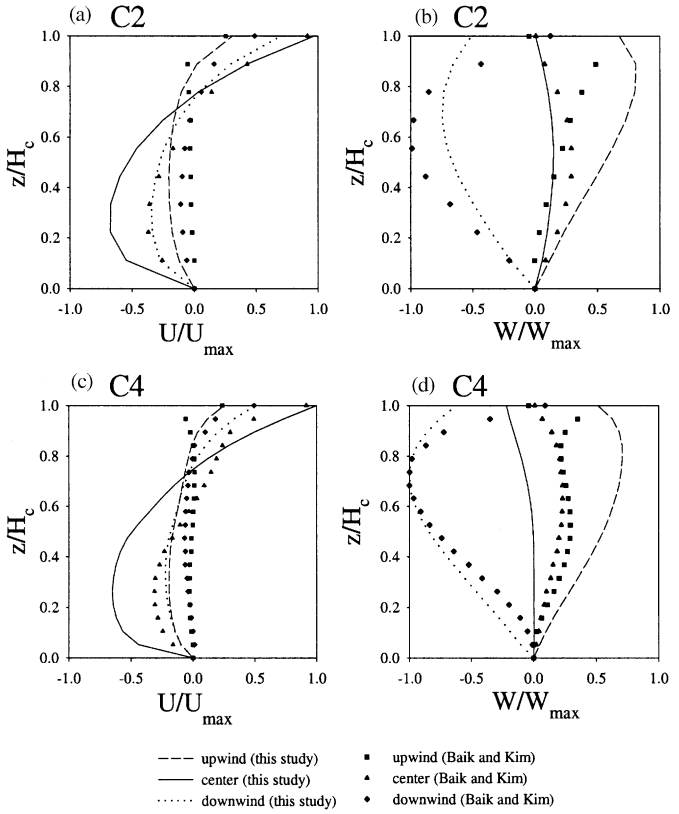

Fig. 5. The vertical profiles of the normalized horizontal and vertical velocities at $t = 2$ h within the street canyon with aspect ratios of 0.44 [(a) and (b)] and 0.93 [(c) and (d)]. The upwind, center, and downwind locations are $x = 350.5, 361.7$, and 370.9 m, respectively.

street-canyon case is stronger than that in the closed street-canyon case (Figs. 5a and c). This is probably because in the open case momentum transfer into the street canyon by the ambient wind is larger than that in the closed case. Such momentum transfer can take place through two processes. The first process is related to the different length of streamline along which momentum transfer from the ambient wind into the vortex occurs. It is thought that momentum is transferred to the vortex along separated streamlines. As the vortex extent exceeds the roof-level, the boundary length between the ambient wind and the vortex in the open case becomes longer than that in the closed case. The second process is associated with wind shear above the street canyon. In the closed case, it was assumed that the wind velocity above the height of 10 m from the roof-level is constant at the inflow boundary. The wind shear above the street canyon in the open case is relatively strong because of a deviation of the ambient wind at the leading edge of the upwind building. Hence, relatively large amount of momentum is transferred to the vortex from the ambient

wind in this open case. As a result of the excess of the vortex extent, the height of vortex center also increases by a factor of 1.15 in the C2 case and 1.28 in the C4 case.

Now, we examine flow field when both a single hill and two buildings are present. Fig. 6 shows the streamline fields in the presence of a single hill with a maximum hill slope of 15.8° and two buildings with aspect ratios of 0.23, 0.44, 0.67, and 0.93

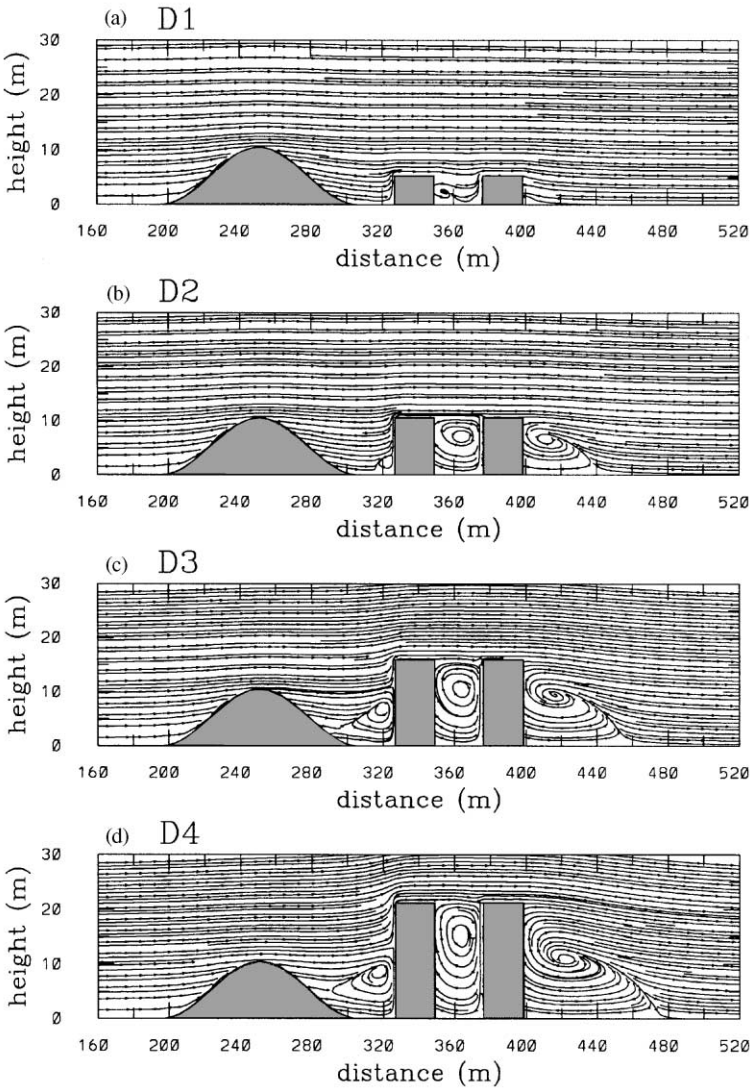

Fig. 6. The streamline fields at $t = 2$ h in a dual-obstacle configuration (a single hill and two buildings) with a maximum hill slope of 15.8° and aspect ratios (H_c/W_c) of (a) 0.23 (D1), (b) 0.44 (D2), (c) 0.67 (D3), and (d) 0.93 (D4).

(denoted by D1, D2, D3, and D4, respectively). Note that in the D2 case the height of hill crest is equal to that of buildings. As in the H1 case (Fig. 2a), a recirculation zone behind the hill is not observed. The circulation between the hill and the upwind building in Figs. 6c and d is generated not by the hill but by the upwind building (see Fig. 4). This circulation might be identified as the horseshoe vortex which is formed below a stagnation point in the presence of inflow wind shear [8]. In three dimensions, it wraps around a building and trails off downwind.

One of the important phenomena resulting from an upwind hill is a variation of the ambient wind above the street canyon (Fig. 7). The horizontal velocity (Figs. 7a and c) is slightly strong in the dual-obstacle cases. A variation of the vertical velocity (Figs. 7b and d) is largest at $x = 322.8$ m in the single street-canyon case with an aspect ratio of 0.44 (Fig. 7b). The difference in the vertical velocity between the C2 and D2 cases is larger than that between the C4 and D4 cases, except at the location of $x = 361.7$ m. The smaller difference in height between the hill and the street canyon results in more effective flow reattachment above the roof-level of the street canyon because the flow deviation by the impingement on the upwind building is weaker. Passing over the upwind hill with the same height as the downwind street

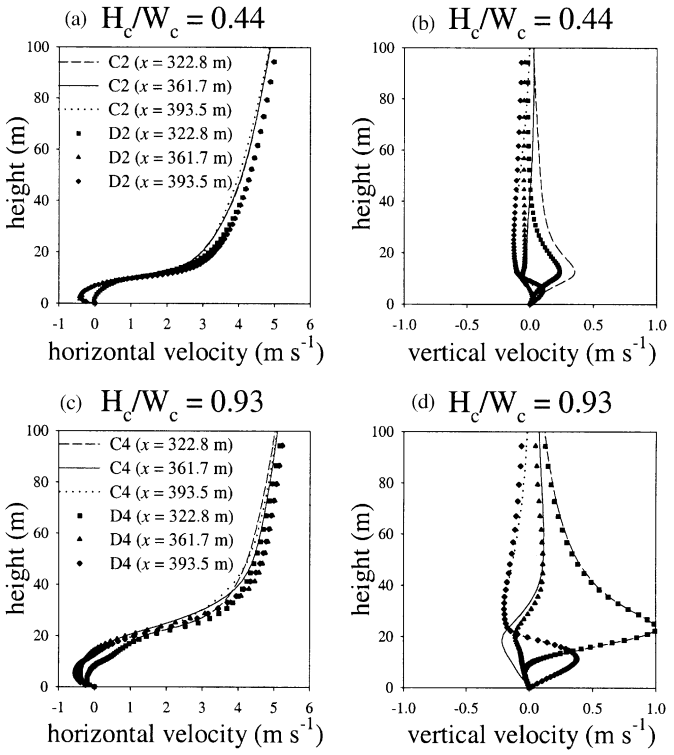

Fig. 7. The vertical profiles of the horizontal and vertical velocities at $x = 322.8, 361.7$, and 393.5 m for aspect ratios of 0.44 [(a) and (b)] and 0.93 [(c) and (d)]. These are C2, C4, D2, and D4 cases and at $t = 2$ h.

canyon in the D2 case, flow reattaches more quickly above the street canyon. As a result, the flow deviation by the impingement on the building is reduced and the vertical velocity at the top height of the canyon approaches zero. This feature is especially noteworthy in that the reattachment promoted by the upwind hill acts to restrict the vertical extent of the vortex below the roof-level. Fig. 6 reveals that there is a distinct increase in the horizontal length of recirculation zone by the upwind hill, except for the D1 case with virtually no increase in the horizontal length. The horizontal lengths of recirculation zone induced by a single street canyon in the C2, C3, and C4 cases are $3.7H_c$, $3.5H_c$, and $3.3H_c$, respectively. In the presence of the upwind hill, the horizontal lengths of recirculation zone increase to $4.0H_c$ (41 m), $3.7H_c$ (57 m), and $3.6H_c$ (77 m), respectively. This indicates that the horizontal length of recirculation zone is affected by the upwind hill whose height is equal to or lower than the street-canyon height.

In the dual-obstacle cases (Fig. 6), an interaction between a recirculation zone behind the hill and a vortex in front of the upwind building is not observed because a recirculation zone is not generated by the upwind hill. For the purpose of examining the interaction, a hill with a maximum slope of 31.3° instead of a maximum slope of 15.8° is placed and four supplementary experiments are conducted. The hill is located at the upwind region of canyons with aspect ratios of 0.23, 0.44, 0.67, and 0.93 (denoted by S1, S2, S3, and S4, respectively). The distance between the hill center and the street-canyon center is the same as in the dual-obstacle cases (that is, 106.6 m). Fig. 8 shows the streamline fields in these experiments. As the height of the canyon increases, the downward motion under a stagnation point which appears on the upwind wall of the upwind building becomes strong and the size of the vortex in front of the upwind building increases. The growth of the vortex influences recirculation zone and in the S4 case the recirculation zone and the vortex in front of the upwind building are combined to yield a horizontally elongated vortex flow.

3.2. Dispersion analyses

Here, we examine pollutant dispersion characteristics in the presence of obstacles depicted in Fig. 1. For this, the pollutant concentration equation is solved using quasi-steady flow fields (wind and turbulence) at $t = 2$ h. A ground-level pollutant source is located at $x = 190.3$ m. Passive pollutants are released at a rate of 100 ppb s^{-1} from the continuous point source during 1 h. The results presented below are at $t = 1$ h after the concentration equation is numerically integrated.

Fig. 9 shows the vertical standard deviation and average height of pollutant plume in the single-hill cases. The average height ($\bar{z}$) and vertical standard deviation (σ_z) of pollutant plume are defined, respectively, as

$$\bar{z}(x) = \frac{\int c(x,z) z \, dz}{\int c(x,z) \, dz}, \tag{4}$$

$$\sigma_z(x) = \sqrt{\bar{z}^2(x) - (\bar{z}(x))^2}, \tag{5}$$

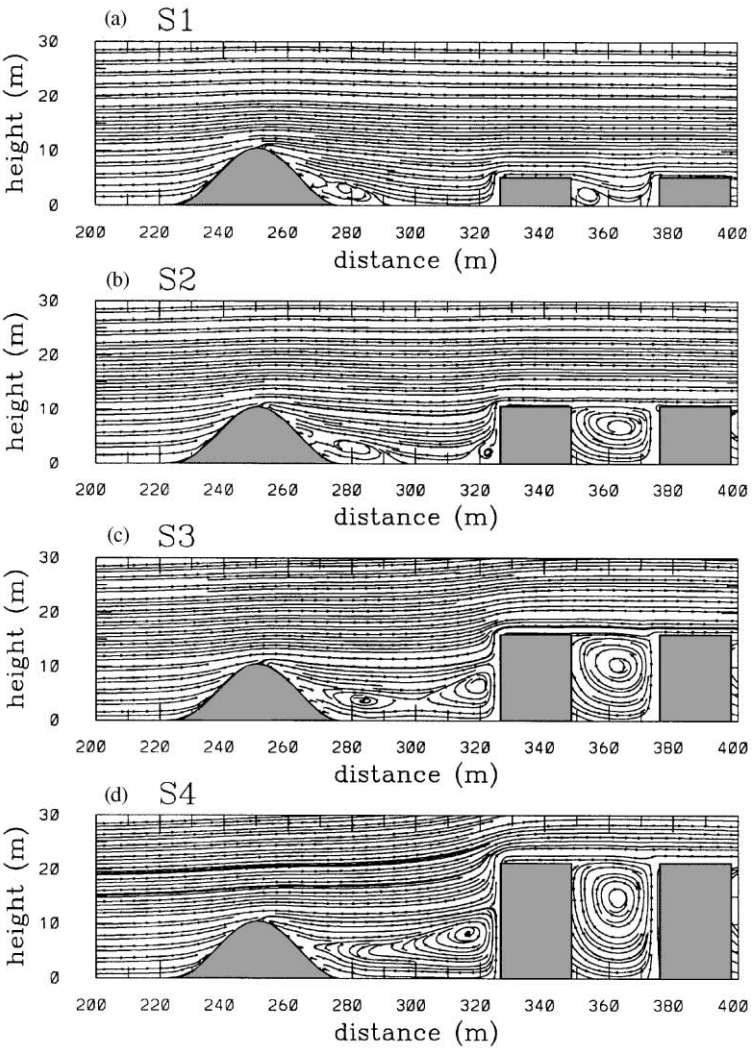

Fig. 8. The streamline fields at $t = 2$ h in a dual-obstacle configuration (a single hill and two buildings with a maximum hill slope of 31.3° and aspect ratios (H_c/W_c) of (a) 0.23 (S1), (b) 0.44 (S2), (c) 0.67 (S3), and (d) 0.93 (S4).

where

$$\bar{z}^2(x) = \frac{\int c(x,z) z^2 \, \mathrm{d}z}{\int c(x,z) \, \mathrm{d}z} \tag{6}$$

with c being the pollutant concentration.

As plume passes over the upwind base and upslope of a hill, the difference in vertical plume spread between the control case (flat bottom case) and each case of

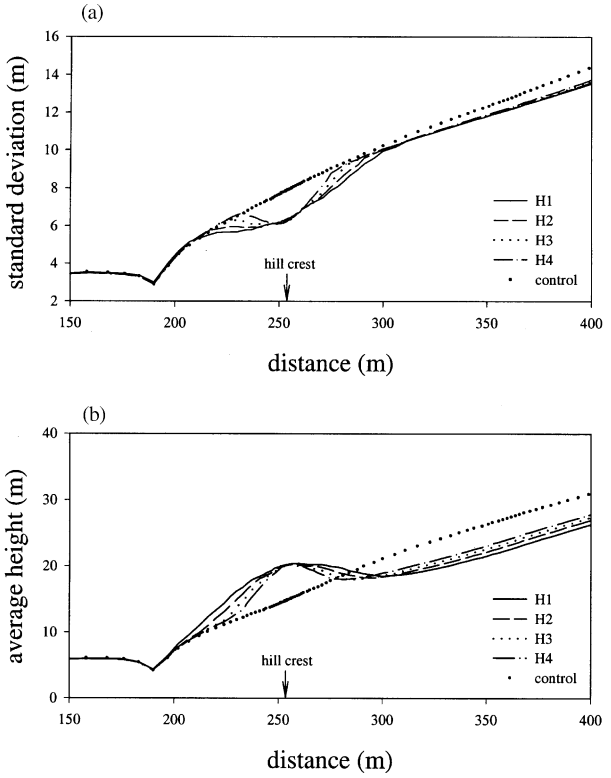

Fig. 9. (a) The vertical standard deviation (σ_z) and (b) average height ($\bar{z}$) of pollutant plume as a function of horizontal distance in a single-hill configuration. The control case (flat bottom case) is also plotted.

the single hills tends to increase and its maximum difference is observed near the hill crest. The difference decreases just behind the hill crest but increases again near the downwind base of the hill. The average plume height increases immediately after plume meets the upwind base of the hill and reaches its local peak near the hill crest. Then, it decreases behind the hill crest but increases again near the downwind base of the hill. Fig. 9 indicates that despite an increase in average plume height, the hill reduces the vertical spread of plume passing over the hill. Downwind of the hill, the average plume height and vertical plume spread are smaller than those in the control case. This is because plume is forced to come down by a widespread downward motion observed downwind of the hill, although it is raised by the upward motion resulting from flow impingement on the upwind slope of the hill. The maximum upward (downward) velocities in the H1, H2, H3, and H4 cases are 0.24 (−0.24), 0.27 (−0.25), 0.32 (−0.28), and 0.37 m s^{-1} (−0.28 m s^{-1}), respectively. As the hill slope increases, downward motion behind the hill becomes stronger but relatively strong upward motion upslope of the hill makes the vertical plume spread and average plume height increase in the downwind region.

The vertical profiles of the pollutant concentration at three locations ($x =$ 322.8, 361.7, and 393.5 m) in the single-hill cases are shown in Fig. 10. In all the cases, the maximum concentration is higher than that of the control case. As the hill slope increases, the maximum concentration decreases but its height increases slightly. The pollutant dispersion is more or less deteriorated by the hill which acts to reduce vertical plume spread and average plume height in the downwind region, although the hill results in plume rise above it.

Fig. 11 shows the vertical standard deviation and average height of plume in the single street-canyon cases. In front of the upwind building, the vertical spread and average height of plume in all the cases, except for the C1 case, are larger than those of the control case. Above the buildings, in comparison with the control case, the average plume height is raised but the vertical plume spread is suppressed. This

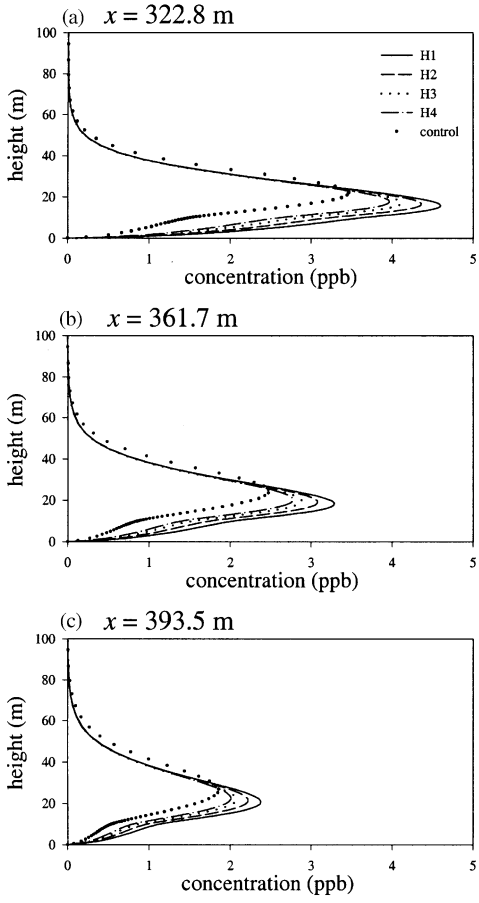

Fig. 10. The vertical profiles of the pollutant concentration at $x =$ (a) 322.8, (b) 361.7, and (c) 393.5 m in a single-hill configuration. The control case (flat bottom case) is also plotted.

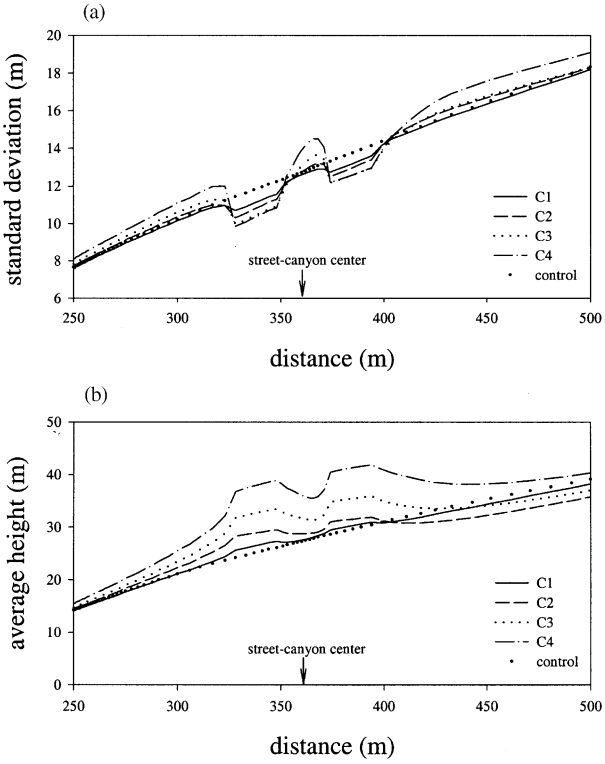

Fig. 11(a),(b). Same as in Fig. 9 except for a single street-canyon configuration. The control case (flat bottom case) is also plotted.

phenomenon also appears when plume passes over a hill (Fig. 9). Above the canyon region (349.1 m$\leqslant x \leqslant$372.3 m), the average plume height in all the cases is raised and the vertical plume spread in all the cases, except for the C1 case, is enhanced. In the downwind region, the average plume height in the C1, C2, and C3 cases becomes lower than that of the control case. This is due to the downward motion induced as flow is reattached to the ground surface in the downwind region. The maximum upward (downward) velocities in front of (behind) the canyon in the C1, C2, C3, and C4 cases are 0.29 (-0.13), 0.68 (-0.21), 1.17 (-0.36), and 1.65 m s^{-1} (-0.40 m s^{-1}), respectively. A weak downward motion in the C1 case results in a high average plume height compared with the C2 and C3 cases.

Fig. 12 shows the vertical profiles of the pollutant concentration near the upwind and downwind buildings within the canyon ($x = 350.5$ and 370.9 m, respectively), on the downwind side of the downwind building ($x = 393.5$ m) and at a downwind location ($x = 500.1$ m). As the building height increases, the maximum concentration is observed at a higher location due to the plume rise by the stronger upward motion. The maximum concentration value in all the cases, except for the C1 case,

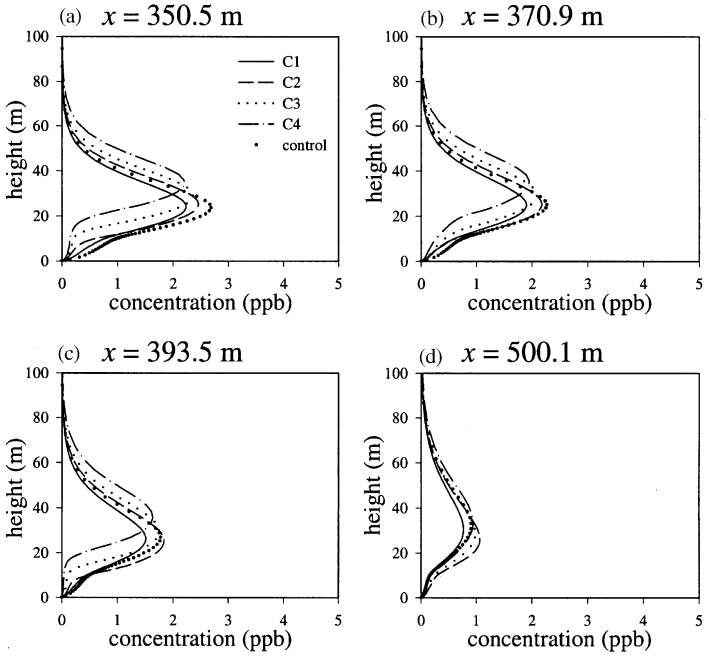

Fig. 12. The vertical profiles of the pollutant concentration at $x =$ (a) 350.5, (b) 370.9, (c) 393.5, and (d) 500.1 m in a single street-canyon configuration. The control case (flat bottom case) is also plotted.

decreases with increasing building height. Within the canyon, the maximum concentration is lower than that of the control case (Figs. 12a and b). In the far-downwind region, the maximum concentration in the C2, C3, and C4 cases is higher than that of the control case (Fig. 12d) due to the widespread downward motion there.

The dual-obstacle cases are shown in Fig. 13. This figure clearly explains upwind hill effect on the vertical spread and average height of plume. As in Fig. 9, the upwind hill enhances average plume height above the hill. However, when plume passes over the canyon, the vertical plume spread and average plume height are reduced in comparison with those in the presence of a single street canyon. This reduction is related to the flow reattachment accelerated by the upward hill above the canyon. As discussed above, the upward hill promotes flow reattachment at the roof-level of the canyon. Accordingly, the flow deviation due to the impingement on the upwind building is reduced (Fig. 7). As a result, the vertical plume spread and average plume height are reduced.

Fig. 14 shows the vertical profiles of the pollutant concentration at the same locations as in Fig. 12. A reduction in vertical plume spread and average plume height due to the upwind hill results in a decrease in pollutant dispersion in the canyon as well as in the far-downwind region. The maximum concentration increases by a factor of 1.9–2.1 compared with those in the presence of a single street canyon.

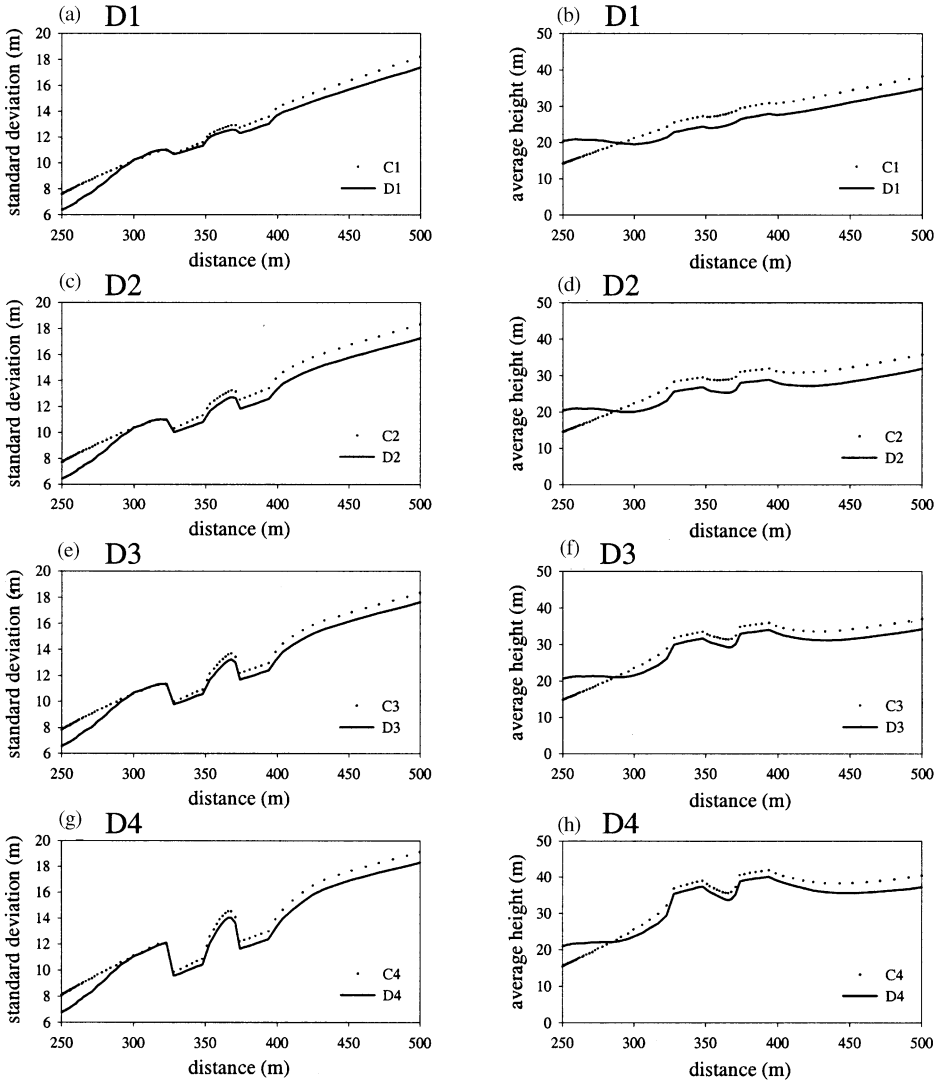

Fig. 13. The vertical standard deviation (a, c, e, g) and average height (b, d, f, h) of pollutant plume in a dual-obstacle configuration in comparison with a single street-canyon configuration.

4. Summary

This study particularly aimed at understanding flow and pollutant dispersion when both a single hill and two buildings forming a street canyon are present. For this, a two-dimensional numerical model which employs a k–ε turbulence closure scheme and a non-uniform grid system was used.

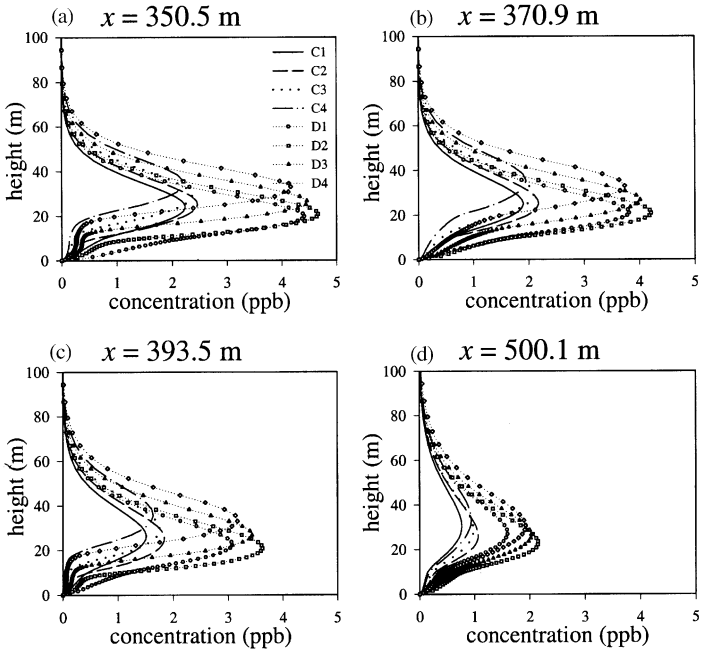

Fig. 14(a)–(d). Same as in Fig. 12 except for a dual-obstacle configuration.

By comparing the results in a single hill or street canyon configuration with those of previous studies, the numerical model used in this study was confirmed to be appropriate in examining the effects of obstacles on mean flow and pollutant dispersion. The mean-flow change was found to be related to both slope and height of an obstacle. A main effect of the hill in front of the street canyon was to accelerate flow reattachment above the street canyon by reducing flow deviation due to the impingement on the building. The flow reattachment promoted by the upwind hill acted to restrict the vertical extent of vortex below the roof-level. Ultimately, it enlarged recirculation zone behind the canyon and decreased pollutant dispersion by reducing the vertical spread and average height of plume above the canyon as well as in the downwind region.

Acknowledgements

The authors are grateful to two anonymous reviewers for providing valuable comments on this study. This work was supported by the Climate Environment System Research Center sponsored by the SRC Program of the Korea Science and Engineering Foundation. This research was also supported by the Brain Korea 21 Program.

References

[1] P.S. Jackson, J.C.R. Hunt, Turbulent wind flow over a low hill, Q. J. R. Meteorol. Soc. 101 (1975) 929–955.
[2] P.A. Taylor, J.L. Walmsley, J.R. Salmon, A simple model of boundary-layer flow over real terrain incorporating wavenumber-dependent scaling, Boundary-Layer Meteorol. 26 (1983) 169–189.
[3] P.J. Mason, J.C. King, Measurements and predictions of flow and turbulence over an isolated hill of moderate slope, Q. J. R. Meteorol. Soc. 111 (1985) 617–640.
[4] S.P.S. Arya, P.S. Gadiyaram, An experimental study of flow and dispersion in the wakes of three-dimensional low hills, Atmos. Environ. 20 (1986) 729–740.
[5] I.P. Castro, A.G. Robins, The flow around a surface-mounted cube in uniform and turbulent streams, J. Fluid Mech. 70 (1977) 307–335.
[6] Y.Q. Zhang, A.H. Huber, S.P.S. Arya, W.H. Snyder, Numerical simulation to determine the effects of incident wind shear and turbulence level on the flow around a building, J. Wind Eng. Ind. Aerodyn. 46&47 (1993) 129–134.
[7] P.J. Mason, R.I. Sykes, On the influence of topography on plume dispersal, Boundary-Layer Meteorol. 21 (1981) 137–157.
[8] Y.Q. Zhang, S.P. Arya, W.H. Snyder, A comparison of numerical and physical modeling of stable atmospheric flow and dispersion around a cubical building, Atmos. Environ. 30 (1996) 1327–1345.
[9] S.P. Arya, Air pollution meteorology and dispersion, Oxford University Press, New York, 1999.
[10] J.-J. Baik, J.-J. Kim, A numerical study of flow and pollutant dispersion characteristics in urban street canyons, J. Appl. Meteorol. 38 (1999) 1576–1589.
[11] S.V. Patankar, Numerical heat transfer and fluid flow, McGraw-Hill, New York, 1980.
[12] L.J. Hunter, I.D. Watson, G.T. Johnson, Modelling air flow regimes in urban canyons, Energy Bldg. 15–16 (1990/91) 315–324.
[13] L.J. Hunter, G.T. Johnson, I.D. Watson, An investigation of three-dimensional characteristics of flow regimes within the urban canyon, Atmos. Environ. B 26 (1992) 425–432.
[14] J.F. Sini, S. Anquetin, P.G. Mestayer, Pollutant dispersion and thermal effects in urban street canyons, Atmos. Environ. 30 (1996) 2659–2677.
[15] I.P. Castro, D.D. Apsley, Flow and dispersion over topography: a comparison between numerical and laboratory data for two-dimensional flows, Atmos. Environ. 31 (1997) 839–850.
[16] R.E. Britter, J.C.R. Hunt, K.J. Richards, Air flow over a two-dimensional hill: studies of velocity speed-up, roughness effects, and turbulence, Q. J. R. Meteorol. Soc. 107 (1981) 91–110.
[17] I.P. Castro, W.H. Snyder, A wind tunnel study of dispersion from sources downwind of three-dimensional hills, Atmos. Environ. 16 (1982) 1869–1887.
[18] S.P.S. Arya, M.S. Shipman, An experimental investigation of flow and diffusion in the disturbed boundary layer over a ridge—I. Mean flow and turbulence structure, Atmos. Environ. 15 (1981) 1173–1184.
[19] T.R. Oke, Street design and urban canopy layer climate, Energy Bldg. 11 (1988) 103–113.
[20] E.-H. Im, J.-I. Han, W.-G. Eom, Three-dimensional numerical simulation to evaluate the effects of incident wind shear and the aspect ratio on the flow around the buildings, J. Korean Meteorol. Soc. 32 (1996) 303–313 (in Korean).